SAFETY CHALLENGES RELATED TO THE USE OF HYDROGEN/NATURAL GAS BLENDS IN GAS TURBINES

Lecocq, G. [1], Proust, C.[12], Leprette E. [1], Daubech, J.[1], Montagne, P[3], Impellizzeri E. [3], Biehler P.[3], Patula P. [3], Auvray, A.[123]

[1] Institut National de l'Environnement Industriel et des Risques, Parc Technologique ALATA, BP 2, Verneuil-en-Halatte, 60550, France

[2] Sorbonne Universités, UTC-TIMR, 1 rue Dr Schweitzer, Compiègne, 60200, France

[3] GE Energy Product France, 20 avenue du maréchal Juin, Belfort, 90000, France

ABSTRACT

In a context of the decarbonization of the power sector, the gas turbine manufacturers are expected to handle and burn hydrogen or hydrogen/natural gas mixtures. This evolution is conceptually simple in order to displace CO_2 emissions by H_2O in the combustion exhaust but raises potential engineering and safety related questions. Concerning the safety aspect, the flammability domain is wider and the laminar flame speed is higher for hydrogen than for natural gas. As a result, handling fuels with increased hydrogen concentration should a priori lead to an increased the risk of flammable cloud formation with air and also increase the potential explosion violence.

A central topic for the gas turbine manufacturer is the quantification of the hydrogen fuel content from which the explosion risk increases significantly when compared with the use of natural gas.

This work will be focused on a risk study of the fuel supply piping of a gas turbine in a scenario where mixing between fuel and air would occur. The pipes are a few dozens of meters long and show singularities: elbows, connections with other lines … They are operated at high temperature and atmospheric or high pressure.

The paper will first highlight through CFD modelling the impact of increasing hydrogen content in the fuel on the explosion risk, based on a geometry representative of a realistic system. Second, the quantification of the explosion effects will be addressed. Some elements of the bibliography relative to flame propagation in pipes will be recalled and put in sight of the characteristics of the industrial case.

Finally, a CFD model proposed recently for accounting for methane or hydrogen flames propagating in long open steel tubes was used to assess a hydrogen fuel content from which the flame can strongly accelerate and generate significative pressure effects, for a flammable mixture initially at atmospheric conditions.

1.0 INTRODUCTION

Decarbonization of the global economy may impose increased use of hydrogen in systems initially configured to use with fossil fuels for producing energy. Among these systems can be counted the gas turbines (GT). They can be used to producing electricity from the combustion of natural gas. GT manufacturers currently offer their products and the associated plants to enable the combustion of natural gas/hydrogen blends in addition to operation on 100% natural gas. There are challenges that can arise when using hydrogen and natural gas blends in systems that were initially configured to operate on 100% natural gas.

The risk management evolution is one of these, notably concerning the explosion risk related to the unwanted formation of fuel/air mixtures in the accessories around the GT. GT manufacturers performed risk analyses related to the use of natural gas and configured their systems for the pressure loads required to meet safety codes and requirements for explosion scenarios involving this fuel. With natural gas/hydrogen blends, all other things being equal (initial pressure and temperature, equivalence ratio …) when compared with pure natural gas, the GT manufacturers have to deal with wider explosion limits

[1,2], *i.e.,* flammable mixtures that can form at lower concentration of fuel in air and higher concentration of fuel in air (on a volume basis) hence ultimately trigger larger flammable clouds, the latter being the volume filled with a fuel/air mixture contained within LFL and UFL. Furthermore, the introduction of hydrogen also leads to mixtures with a higher laminar flame speed [3] than for pure natural gas. Both trends correspond to a potential increase of the pressure load. This effect is slightly counter balanced by a reduction of the thermal expansion rate for natural gas/hydrogen blends. This quantity measures the increase of the burned gases volume compared with the fresh gases one. It partly drives the maximum pressure that can be reached in a confined explosion.

Thus, the explosion risk evolves with the introduction of hydrogen in their systems for GT manufacturers. A central issue is the amount of hydrogen that can be used in the blends without significantly changing the pressure loads associated with the use of 100% natural gas.

The current study focuses on a part of the fuel circuit upstream the gas turbine. This part is made of a long pipe, the header, of approximately 10 meters long, that feeds a distribution ring manifold around the GT dispatching the fuel to each combustion chamber via several short pipes. The present study is aimed to evaluate a scenario where fuel and air would have mixed unintendedly in this system, at high pressure and temperature.

First, modelling is performed for characterizing the flammable volumes that can be formed for several hydrogen/methane in air blends in the long pipe. Methane is considered as a substitute of natural gas to simplify the calculation. Second, the way pressure effects could be estimated is considered. Some elements of the bibliography specific to the identified flammable volumes are then recalled and some engineering models are tested against experimental results. The lack of knowledge and simple methods for quantifying the pressure effects in realistic systems is then highlighted. Finally, a CFD study is carried out in order to assess a threshold for the hydrogen fuel content in volume fraction, $\boldsymbol{\alpha_{H2}}$, for the case of atmospheric flames propagating in long tubes, from which quick flames could be obtained.

2.0 MODELLING THE FLAMMABLE VOLUME FORMATION

A simplified geometry of the studied portion of the circuit upstream the GT combustion chambers is shown in the Figure below. In fact, some elements of the real geometry (two elbows and one diameter reducer) were removed. Only half of the geometry is presented, the other one could be deduced by reflection across a central symmetry plane.

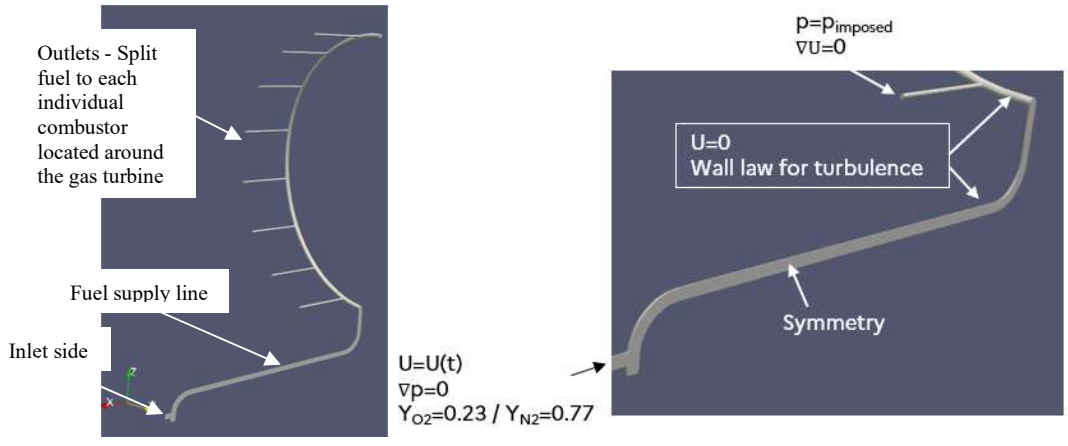

Figure 1. Computational domain (left) and boundary conditions (right).

The main line is about 20 m long piping with a diameter of approximately 100mm (4’’). It includes singularities: elbows, tees, and connections through smaller diameter tubes with the several combustion chambers.

In the operating point of interest, the line is initially filled with a fuel at a temperature of about 300°C and a pressure of about 25 barg. Then a contact between fuel and air can be enabled, at a temperature of about 250°C. It should be noted these three values are orders of magnitude for reference only. Fuels which were studied are natural gas or a natural gas/hydrogen blend, as well as low calorific steel mill gases (Blast Furnace Gas; Coke Oven Gas mixture).

At this point, it is assumed that a mixing layer can be initiated in the process at the inlet. It will be pushed by the inlet flow and will evolve, in terms of thickness and distribution in space, until reaching the outlets of the domain. A flammable volume is likely to be created with the mixing layer.

Lower Flammability Limits (LFL) and Upper Flammability Limits (UFL) have to be quantified for the hydrogen/methane/air mixtures and the thermodynamic conditions of interest. The data used in defining the flammability limits in this study are summed up in the Table below. According to the data, LFL of methane seems to weakly depend on pressure when this latter is lower than 30 bar. The same is true for hydrogen. The LFL being known for the operating temperature for hydrogen and methane, the LFL of H_2-CH_4 blends can be deduced using the Le Chatelier formula [4]. This formula is not used in practice for quantifying UFL because it is not accurate enough [5]. In order to fill the gap between the available data in bibliography for UFL of H_2-CH_4 blends and the studied operating point, it is proposed to tune the Le Chatelier law according to references [1,6,2]. To do so, two assumptions are used: 1) the data proposed by Vanderstraeten [7] can be linearly extrapolated until 300°C, 2) the UFL of hydrogen weakly depends on pressure until 30 bar.

Table 1. Database for the quantification of LFL and UFL for the mixtures of interest. α_{H2} is a volume fraction of hydrogen in the fuel.

Fuel	Studied flammability limit	Investigated range	Ref.
CH_4	LFL	T_u = 25-300°C / P=1bar	[8]
CH_4	LFL	T_u = 20°C / P=1-100bar	[1]
CH_4	UFL	T_u = 20-200°C / P=1-55bar	[7]
H_2	LFL-UFL	T_u = 20-400°C / P=1bar	[6]
H_2	LFL-UFL	T_u = 20°C / P=1-150bar	[1]
CH_4 / H_2	LFL-UFL	T_u = 20°C / P=1-100bar / α_{H2}=0-100 %	[1]
CH_4 / H_2	UFL	T_u = 20-200°C / P=1bar / α_{H2}=0-100 %	[6]
CH_4 / H_2	UFL	T_u = 20-200°C / P=1-10bar / α_{H2}: 20 or 40%	[2]

It was chosen to characterize through CFD the flammable clouds that can be obtained for fuels being pure methane or pure hydrogen and a hydrogen/methane blend with α_{H2}=30 %. The computed flammability limits for the blends and thermodynamic conditions of interest are given in Table 2.

Table 2. LFL and UFL used in the CFD model to delineate the flammable cloud

α_{H2}	LFL	UFL
0 %	3.5 %	49 %
30 %	3 %	72 %
100 %	2 %	91 %

The CFD code used in this study is OpenFoam v1912 [9]. It is used for solving the RANS-averaged transport equations of momentum, pressure, mass fractions of the chemical species and enthalpy. Turbulence is closed with the k-ω SST model [10]. The differential diffusion effects are neglected as well as the buoyancy effects.

The mesh is made of 1.1 million of hexahedra. The main cell width is about 6.3 mm. The mesh is refined at walls with a minimum cell width about 1 mm. The chosen boundary conditions are shown in Fig. 1.

The wall law is the one proposed by Spalding [11], valid both in the linear and in the logarithmic parts of the boundary layer. The y^+ values remained about a few dozens in the main mixing regions.

Figure 2 shows the time evolution for the total flammable volume for the three cases considered. It should be noted the values were normalized by the peak volume reached by case with α_{H2}=100%. It can be seen the same trend is observed in the three cases: a quick increase of the total flammable volume until a maximum is reached at roughly 3 seconds, then a progressive decrease until 7-8 seconds where an asymptotic value is reached. An increase in the hydrogen fuel content leads to an increase in the maximum total flammable volume. Compared with the pure methane case, the 30 % hydrogen case corresponds to an increase of 60 % while the 100 % hydrogen case leads to an almost 3 times larger flammable cloud.

As a complementary example, steel mill gases mixture was considered, containing 22% CO / 15 % CO_2 / 13 % H_2 / 4% CH_4 / 44 % N_2. In this case, due to the high concentration of inert gas, the fuel is weakly reactive. The LFL (17.5%) and UFL (64.6 %) in air were computed thanks to the Bounaceur et al. method [12]. The flammable volume was computed with the CFD using this fuel and put as a comparison to natural gas and hydrogen-enriched natural gas, and clearly highlights the influence of a higher LFL to the flammable cloud size, which is in this case less than twice smaller.

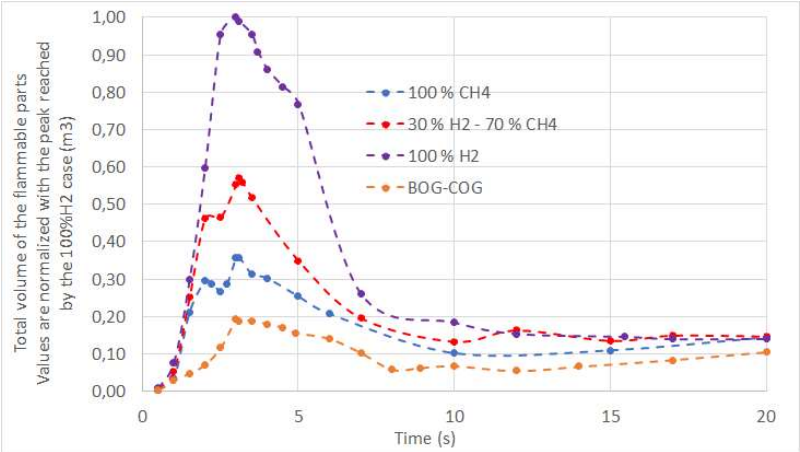

Figure 2. Normalized flammable volumes determined with CFD.

The impact of the geometry was simply investigated by performing the computation carried out for the fuel with 30 % of hydrogen in a straight tube, with an inlet and a single outlet. The length of the straight tube is the same as the main line length in the simplified geometry. All the other parameters are kept equal. Figure 3 shows the absence of singularities (elbows, tees, ring…) in the geometry greatly reduces the size of the flammable volume. This was expected from a qualitative standpoint since singularities will increase the turbulence and mixing capability of the two fluids together and will generate recirculation zones which will make mixture last longer in time duration.

Figure 4 highlights for two close instants the evolution of the flammable cloud position for the fuel for with $\boldsymbol{\alpha_{H2}}$=30 % as well as the equivalence ratio profile inside this cloud. These instants were chosen as the flammable cloud is mainly located in the long straight portion, making easier the post-processing.

It can be seen the flammable volume contains some discontinuity and eventually splits in two portions Also, it does not fully fill the whole (straight pipe) section on its length. This latter trend seems to be related to singularities with which the flammable cloud interacted.

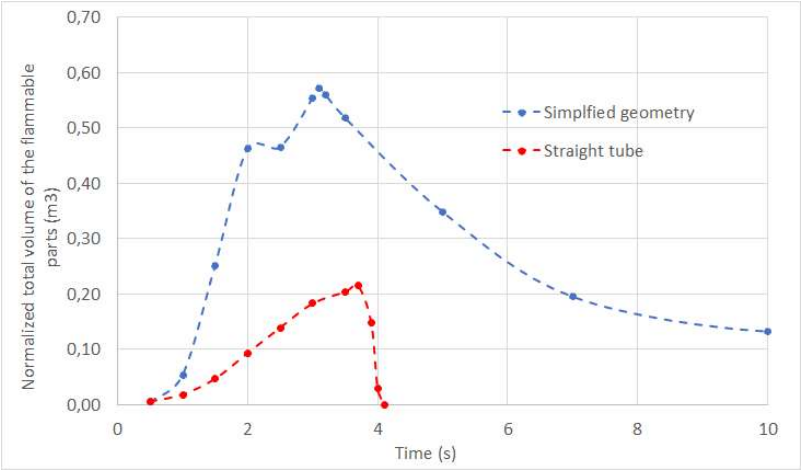

Figure 3. Normalized flammable volumes determined with CFD for a fuel containing 30 % of hydrogen.

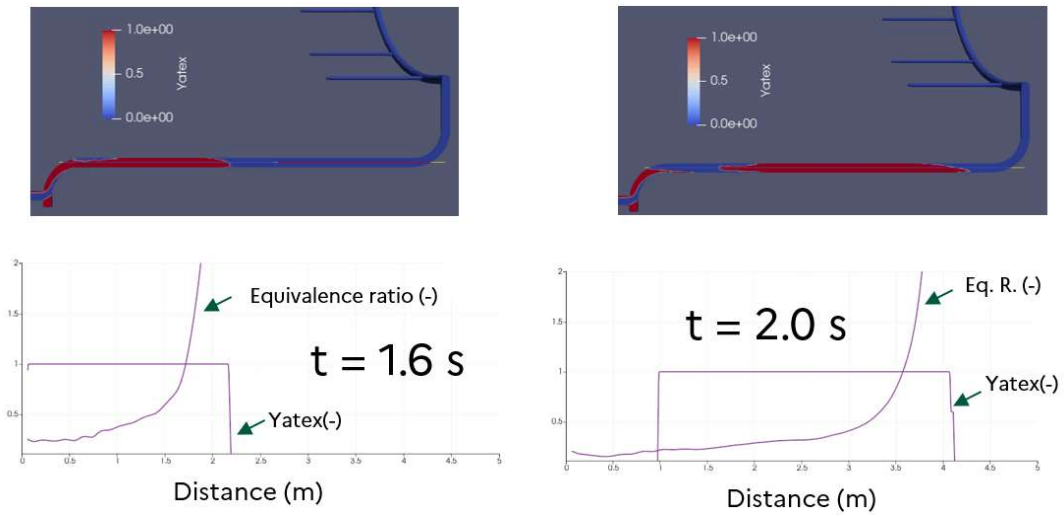

Figure 4. Evolution of the flammable cloud (top) for α_{H2}=30 % between two instants and evolution of the equivalence ratio distribution inside this cloud in the straight portion of the pipe (bottom).

On the longest portion of the flammable cloud, it appears that half the length is made of rather constant and lean equivalence ratio, the other being made of an equivalence ratio gradient, limited by UFL. With the three hydrogen fuel contents modelled, it appeared the same structure of the flammable cloud was recovered in the long portion of the pipe. When the hydrogen fuel content increases, the proportion of the lean portion in the total length increases and the mean equivalence ratio of this part decreases. This trend also leads to a decrease of the mean equivalence ratio of the flammable cloud, which is expected by theory given the higher stoichiometric fuel/air ratio of hydrogen vs natural gas.

3.0 QUANTIFING PRESSURE EFFECTS RELATED TO AN EXPLOSION IN A REALISTIC DEVICE

For the GT manufacturers, if the risk of a flammable cloud formation in the feeding pipes cannot be excluded, it is key to be able to quantify the pressure loading on the system that comes from a potential explosion related to the presence of an ignition source in this cloud in order to eventually size the piping system so that it can withstand such failure mode. Indeed, the resistance of the mechanical elements to all pressure loadings encountered during the lifetime of the system should be ensured.

Explosions of previously identified flammable mixtures (in the fuel supply system) are assumed to have specific parameters:

- the flame would be confined and guided in a steel tube,
- this tube includes singularities: elbows, diameter restrictions, tees …
- the flame would propagate in a mixture initially at high pressure and temperature,
- the fuel can be natural gas, hydrogen, or a mixture of both species with varying relative proportions,
- the flame would propagate in zones with varying equivalence ratios.

Furthermore, an effective length on which the flame could propagate was computed for the three first fuels considered in the previous part. The effect of the mean flow was not taken into account. The "Effective length" accounted for the thermal expansion of the gases *i.e.* the fact the unburned reactant gases were pushed by the flame by the burned ones, increasing the flame propagating length. The maximum expansion of the burned gases could be quantified through the mean thermal expansion ratio of the flammable clouds. In all cases, the quantified effective flame propagation length is of the order of ten meters

Flames in tubes are prone to a continuous acceleration [13]. To the author's knowledge, the equivalence ratio of the flammable mixture is homogenous in the tube and there is no initial flow in the experimental or theoretical studies dedicated to this kind of explosions in the literature. When the ignition occurs at the centre of a closed end, it was shown the flame first develops spherically around the ignition point, is then elongated due to confinement and reaches a maximum surface about $2.\tau.S_{tube}$ where τ is the thermal expansion rate and S_{tube} the tube cross-section area [14]. This first acceleration phase corresponds to the generation of a first pressure peak. It is followed by a second acceleration phase. The acceleration intensity then depends on the flame reactivity [15] (*i.e.,* the quantity $\tau.S_L$ with S_L the laminar flame speed), the tube material and diameter [16]. Some theories explaining the acceleration rely on the assumption of the generation of a turbulent boundary layer between the flame front and the leading train of shocks waves, with an interaction of the flame front with the more and more intense turbulence close to the walls [17]. Other physical effects promoting flame acceleration can be at stake, such as the instabilities effects leading to an increase of the flame front wrinkling. If the flame acceleration is strong and if the flammable cloud is long enough a Deflagration-To-Detonation Transition (DDT) can even be observed.

Explosion experiments were performed in 24 m long, 150 mm wide steel tubes, with one side closed, the other open [18]. The fresh gases are either a stoichiometric methane/air mixture or a hydrogen/air lean mixture and ignition is triggered at the closed side. This set-up shows many similarities with the industrial case, namely diameter and length of the pipe. Two distinct behaviours were observed: a deflagration for the methane flame, a DDT for the hydrogen case.

Examining existing reference, a limited data set was found for fuels mixing hydrogen and methane, but the tubes were rather short for enabling significant flame acceleration [19-20]. Another work [21] was dedicated to the experimental study of the distances at which DDT occurred in tubes (*run-up distances*). The set-up comprised a Shchelkin spiral for promoting flame acceleration, a helical section and straight tube. The authors observed the run-up distance was not varying monotonically with the fuel enrichment in hydrogen, but this behavior might be related to the design of the tube, according to them.

Most experiments in straight tubes were carried out for a flammable mixture initially at room temperature and atmospheric pressure. An experiment [22] was nevertheless found for which the unburned reactant gases temperature was varied from 300 to 650 K, in a 21.3 m long and 27.3 cm wide tube that contained regularly spaced rings. The fuel was hydrogen. It was observed the rate of initial

flame acceleration decreased and distances at which DDT occurred (run-up distance) increased when the temperature increased. According to the authors, the first trend could be due to an increase of the fresh gases viscosity, the second one to an increase of the speed of sound in fresh gases. This latter increase could require a longer time to form a shock wave and delay DDT. The conclusions may be specific to the studied configuration though.

Some data can be found for initially pressurized mixtures [17,23-24] and long tubes. Reference [17] clearly shows the run-up distance decreases when the initial pressure increases. In the other works, too many parameters were varied, and a clear conclusion is difficult to obtain.

Thus, for the simplified case of a smooth steel tube, data can be found that account for the effect of a few specificities of the industrial explosion. Nevertheless, it appears tricky to anticipate the behaviour of a known experimental flame for which multiple parameters (for example: initial pressure and temperature) would be changed. A dataset showing a sufficient crossing of the key parameters (hydrogen fuel content variation, equivalence ratio, initial temperature, initial pressure) seems to be missing in the literature. Nevertheless, there are a few engineering models available [25-26]. Dorofeev et al. [25] accounted for a mass conservation equation across the tube section. They also used the Bradley correlation [27] for closing the turbulent flame speed S_T appearing in this equation. When the flame propagates at a speed close the speed of sound in the burnt gases, the chocked regime is reached. Assuming DDT occurs soon after, the following expression is proposed to quantify the run-up distance X_{DDT} ($\sim X_S$):

$$\frac{X_S}{D} = \frac{\gamma}{C}\left(\frac{1}{\kappa}\ln\left(\gamma\frac{D}{h}\right) + K\right) \text{ with } \gamma = \left(\frac{a_p}{\eta(\tau-1)^2 S_L}\left(\frac{\delta}{D}\right)^{\frac{1}{3}}\right)^{\frac{1}{2m+\frac{7}{3}}} \quad (1)$$

This model accounts for the following additional parameters:

- The flammable mixture properties (the thermal expansion rate τ the laminar flame speed S_L and the flame thickness δ).

- The speed of sound in the combustion products a_p.

C, η, κ, K and m are constants. Dorofeev et al. obtained a precision of 25 % when computing the distance X_S for several flames. The model was tested against the experimental cases described in Refs. [16,18]. The input parameters as well as the results are given in Table 3.

According to the model, the methane flame in the 150 mm wide tube is about to reach 1000 m/s when it approaches the end of the tube, while in reality, the flame speed is about 150 m/s at this point. For the same tube, the computed run-up distance for the hydrogen blend is quite close to the real one. Concerning the 250 mm tube, it is difficult to assess the result for the methane flame, the predicted run-up distance being greater than the real tube length. Nevertheless, the measured flame speed toward the end of the tube was about 100 m/s only. The precision of the results for these cases are very different from one to the other. It may also depend on the way the input parameters were computed. The fact the model is valid for open tubes can be questioned.

According to the model, the methane flame in the 150 mm wide tube is about to reach 1000 m/s when it approaches the end of the tube, while in reality, the flame speed is about 150 m/s at this point. For the same tube, the computed run-up distance for the hydrogen blend is quite close to the real one. Concerning the 250 mm tube, it is difficult to assess the result for the methane flame. The precision of the results for these cases are very different from one to the other. It may also depend on the way the input parameters were computed. The fact the model is valid for open tubes can be questioned.

Table 3. Input parameters and result for the Dorofeev et al. model.

Mixture	D (mm)	S_L (m/s)	τ (-)	δ (mm)	a_p (m/s)	h (μm)	X_S (m)	Experimental X_S (m)
10 % CH_4 – 90 % air	150	0.4	7.5	0.04	925	50-150	23-26	Not reached
10 % CH_4 – 90 % air	250						37-42	Not reached
20 % H_2 – 80 % air	150	0.9	5.6	0.02	860		18-20	Between 10 and 15

Silvestrini [26] proposed the following expression for the flame speed evolution in tubes:

$$V_F = A\sigma S_L e^{B(\tau-1)\left(\frac{x}{D}\right)\left(\frac{D}{0.15}\right)^{\beta}} \quad (2)$$

The constants (A, B, β) appearing in this equation are obtained from a fitting with experimental results (hydrogen, propane, methane and ethylene flames propagating in 0.15, 0.25 and 1.40 m wide tubes).

The model for V_F is compared to the experimental results related to hydrogen and methane flames propagating in a 24 m long, 150 mm wide steel tube [18], measured at INERIS, the laboratory of ones of the authors of the present paper. It appears the model does not predict the measured accelerating trends.

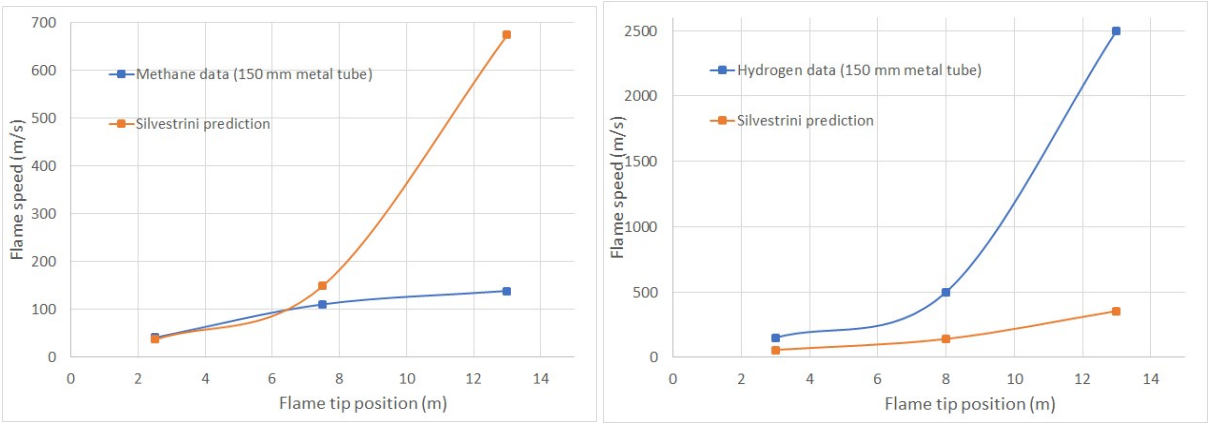

Figure 5. Comparison of the measured and computed flame speeds histories for flames propagating in a 24 m long, 150 mm steel tube. Left: methane flame. Right: hydrogen flame.

To sum up, accounting for the specificities of the industrial case in a "simplified" topology, the straight tube, leads to explosions with a qualitative behaviour which is tricky to predict. Knowledge seems to be missing for characterizing the effects of all the parameters variations. Furthermore, there is no known engineering tool that can model the selected representative cases of the literature.

4.0 EXTRAPOLATIONS OF EXPERIMENTAL RESULTS WITH CFD

As mentioned above, a key point for GT manufacturers is the threshold in hydrogen fuel content that significantly increases the pressure loading if an explosion happened in the system. A first step towards an answer for a flammable volume fully representative of this situation is proposed with the case of a homogeneous flammable mixture contained in a 150 mm wide, 24 m long steel tube previously mentioned. This topology is attractive as the tube diameter is close to one of the set-up of interest. The tube length is also well represented since similar. Also, two extreme flame behaviours were measured (deflagration and DDT).

A previous work [18] was dedicated to the CFD modelling of these cases. It is proposed to exploit this former to extrapolate the threshold in hydrogen fuel content for initial atmospheric pressure and temperature and stoichiometric mixtures. The retained hydrogen fuel contents are: 10, 20, 25, 30, 40, 50 and 75 %.

The transport equations were solved for momentum, pressure, a progress variable and energy with a pressure-based solver of the CFD code OpenFoam v2106. Turbulence was also modelled with a k-ω SST model [28]. The flame front was localized with the gradient of the progress variable. The chemical source term which pilots the propagation speed of the flame front was simply closed as the product of this gradient, the density of the fresh gases (ρ^u) and a characteristic flame front speed: $\bar{\rho}\,\widetilde{\omega_c} = \rho^u S_F |\nabla \tilde{c}|$. The flame speed S_F then wrote: $\Xi . S_L$ where Ξ was a wrinkling factor. This latter was explained as the product of characteristic wrinkling factors, each one accounting for a phenomenon accelerating the flame speed: thermo-diffusive and Darrieus-Landau instabilities, pressure effects, etc.

The wrinkling factor Ξ was closed as: $\Xi = \Xi_t . \Xi_I$ where Ξ_t represented flame wrinkling induced by flame/turbulence interaction and was closed with the turbulent flame speed correlation proposed by Gülder [29]. The wrinkling factor Ξ_I represented the effects of instabilities. Keeping the commonly made assumption of a unitary Lewis number for stoichiometric methane/air flames, Ξ_I was set to 1.0 for this case. An ad hoc value close to 3.4 was chosen for the lean hydrogen-air flame. This value enabled to recover the measured flame acceleration. The wrinkling factor Ξ_I is closed as follows for varying hydrogen fuel contents and assuming stochiometric mixtures:

$$\Xi_I = 3.4\ (\alpha_{H2}) + 1.0\ (1 - \alpha_{H2}) \quad (3)$$

The laminar flame speed for all H_2/CH_4 is considered as constant with pressure and temperature. The values that are used in the previous and current works come from the experimental work of Salzano et al. [27]. They are given in the Table below.

Table 4. Laminar flame speed used for the CFD modelling for stoichiometric mixtures. *Case of the H_2/air lean mixture.

% vol. H2	0	10	20	25	30	40	50	75	100*
S_L (m/s)	0.4	0.55	0.67	0.72	0.77	0.9	1.06	1.54	0.9

The computational domain is limited to the part of the pipe filled by the flammable mixture. At walls, velocity is zero and turbulent viscosity is modelled with a wall law. At the outlet plane, the pressure is set to the atmospheric pressure and the velocity gradient is set to 0.

The walls are assumed to be adiabatic (temperature gradient set to 0). The steel roughness is assumed to be around 150 µm which corresponds to a weakly rusted steel. This characteristic is used in the wall laws.

The 3-D mesh is made of 2.5 million hexahedra, with 36 cells in the tube diameter. The maximum characteristic cell width is about 6 mm. The time derivative is discretized with a first order (Euler) scheme while second orders schemes are used for the convection and diffusion operators. There is no specific procedure for capturing the shocks.

The Figures 6 and 7 show the evolution of the computed flames' position with time as well as the pressure signal obtained 16 m away from ignition point.

The progressive flame acceleration with the hydrogen fuel content can be seen in Figure 6. When there is no hydrogen in the fuel, a flame deflagration is observed with two main peaks, the first one at 100 ms being related to the initial flame elongation, the second one (t ~ 220 ms) corresponding to the end of the following acceleration phase.

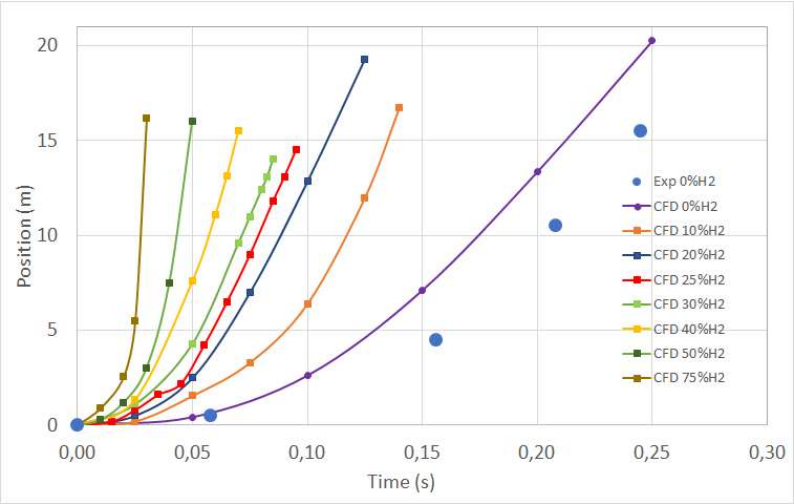

Figure 6. Dotted-lines: computed flame tip position for several hydrogen-methane-air mixtures in a 24 m, 150 mm wide, steel open tube. Dots: experimental flame position with α_{H2}=0 %, each dot corresponding to a measuring point.

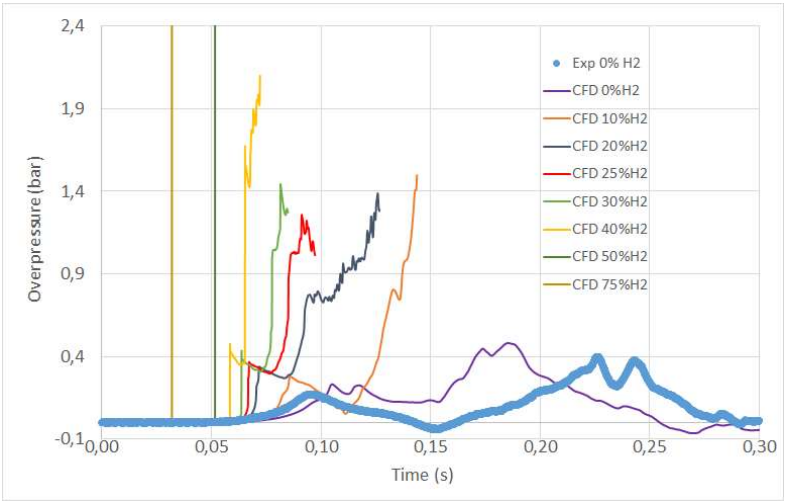

Figure 7. Lines: computed pressure signals for the hydrogen-methane-air mixtures in a 24 m, 150 mm wide, steel open tube. Dots: experimental flame position with α_{H2}=0 %. Signals obtained at 16 m from ignition point. Peak computed pressures for α_{H2}=50 % and α_{H2}=75 %: 60 and 30 bar.

With an increase of the hydrogen fuel content, the first pressure peak steepens and the second one reaches higher values than the one obtained with α_{H2}=0 %. Also, the time delay between the two pressure rises decreases. The first pressure rise becomes a shock for α_{H2}=25 %. The signals obtained for α_{H2}=50 % and α_{H2}=75 % show a single shock with a very high magnitude (dozens of bars). The magnitude of the shock is not the highest for the case with α_{H2}=75 % which seems contradictory with theoretical physics. Actually, the chosen modelling only represents an accelerating turbulent flame. The physics related to detonation are not taken into account, which limits accuracy of the prediction for the detonation phase. The model was applied here to attempt to detect key hydrogen fuel content thresholds.

Considering fast flames are encountered as soon as shocks can be formed, it seems that for this experimental set-up this transition is observed for α_{H2}=25 %. The qualitative results also indicate that a DDT could occur for α_{H2}=50 %.

5.0 CONCLUSIONS

GT manufacturers are expected to burn new fuels in their system, such as natural gas/hydrogen mixtures and other hydrogen containing fuels and attach a significant care to the new risks assessment which come with this fuel switch

It first appeared realizable to characterize the flammable cloud properties (volume, equivalence ratio) for several fuels and assess the impact of hydrogen addition in the fuel, through CFD modelling.

Predicting the pressure effects seems more complex. Flame in tubes show acceleration specificities, with some of them being described in the literature. While some qualitative trends of the specificities of the industrial case such as high pressure and temperature effects can be found in the literature, data remain limited and experimental results related to cross variations of these parameters were not found.

In the framework of an ongoing PhD thesis involving INERIS, GE and UTC, it is planned to design and build a large, closed tube enabling to study flame acceleration for hydrogen-methane-air mixtures at high temperature and pressure. This work is expected to bridge a gap in data and knowledge needed to address properly explosion cases in real industrial systems.

Also, some engineering models for predicting flames in tube propagation were tested and some limits were identified.

Finally, a CFD approach was tested for extrapolating experimental results to other hydrogen fuel contents, in order to see if characteristic thresholds could be identified.

6.0 REFERENCES

1. Pahl R., Bestimmung der Explosiongrenzen von Wasserstoff/Methan-Gesmischen bei höheren Anfangsdrücken, Diplomatarbeit Technische Fachhochschule Berlin (1994), durchgeführt in der BAM
2. Van den Schoor F., Influence of pressure and temperature on flammability limits of combustible gases in air, PhD thesis, 2007
3. Salzano E. et al. Explosion behavior of hydrogen-methane/air mixtures. J. Loss Prev. In the Process Ind. 25, 2012, pp. 443-447
4. Le Chatelier H., Boudouard O., Sur les limites d'inflammabilité des mélanges gazeux. Bulletin de la société chimique de Paris 19, 1898, pp. 483-488
5. Kondo S. et al. A study on flammability limits of fuel mixtures. Journal of Hazardous Materials, 155, 2008, pp. 440-448
6. Gasse A., Experimentelle Bestimmung und Simulation von Explosionsgrenzen, untersucht an wasserstoffhaltigen Brenngasgemischen, Disseration Universität-Geasmthochscule Padeborn, Reihne Verfahrenstechnik, Shaker, Aachen, 1992
7. Vanderstraeten B. et al., Experimental study of the pressure and temperature dependence on the upper flammability limit of methane/air mixtures, Journal of Hazardous Materials 56, 1997, pp. 237-246
8. Wierzba I. et al., The flammability limits of H2-CO-CH4 mixtures in air at elevated temperatures, International Journal of Hydrogen Energy 31, 2006, pp. 485-489
9. www.openfoam.com
10. F.R. Menter, M. Kuntz, and R. Langtry, Ten years of industrial experience with the SST turbulence model. In *Proceedings of the fourth international symposium on turbulence, heat and mass transfer*, 2003, pp. 625–632, Antalya, Turkey. Begell House
11. Spalding D.B., A single formula for the law of wall. – J. Appl. Mech., vol.28, Ser. E, 1961, pp.455-458

12. Bounaceur R., Glaude P.-A., Sirjean B., Fournet R., Montagne P. Vierling M., Moliere M., Prediction of auto-ignition temperatures and delays for gas turbines applications. Journal of Engineering for Gas Turbines and Power, American Society of Mechanical Engineers, 2016, 138, pp. 021505
13. Cicarelli G. and Dorofeev S., Flame acceleration and transition to detonation in ducts. Progress in Energy and Combustion Science 34, 2008, pp. 499-550
14. Bychkov V., Akkerman V., Fru G., Petchenko A., Eriksson L.-E., Flame acceleration in the early stages of burning in tubes. Combust. Flame 150, 2007, pp. 263-276
15. Proust C., Gas flame acceleration in long ducts. Journal of Loss Prevention in the Process Industries 36, 2015, pp. 387-393
16. Daubech J., Leprette E., Proust C., Lecocq G. Further insight into the gas flame acceleration mechanisms in pipes. Part I: Experimental work. Journal of Loss Prevention in the Process Industries 62, 2019, pp.art. 103930
17. Kuznetsov et al. DDT in a smooth tube filled with a hydrogen-oxygen mixture. Shock Waves 14(3), 2005, pp. 205-215
18. Lecocq G., Daubech J., Leprette E., Experimental and numerical study of the fuel effect on flame propagation in long open tubes, Journal of Loss Prevention in the Process Industries 81, 2023, pp.art. 104955
19. Yu M. et al., Effects of hydrogen addition on propagation characteristics of premixed methane/air flames. J. Loss Prev. In Process Industries 34, 2015, pp. 1-9
20. Yu M. et al., Scale effects on premixed flame propagation of hydrogen/methane deflagration. Int. J. of Hydrogen Energy 40, 2015, pp. 13121-13133
21. Shamshin I.O., Kazachenko M.V., Frolov S.M., Basevich V.Ya, Deflagration-to-Detonation transition in stochiometric mixture of the binary methane-hydrogen fuel with air. 2021. Int. J. of Hydrogen Energy 46(68), pp. 34046-34058
22. G. Ciccarelli, J.L. Boccio, T. Ginsberg, C. Finfrock, L. Gerlach, The effect of initial temperature on flame-acceleration and deflagration-to-detonation transition phenomenon. 1998. NUREG/CR-6509. BLN-NUREG-52515
23. Shildberg et al., Experimental Determination of the Static Equivalent Pressures of Detonative Explosions of Stoichiometric H2/O2/N2-Mixtures in Long and Short Pipes, Proceedings of ASME 2015 Pressure Vessels and Piping Division, Conference ASME/PVP, Boston, Massachusetts, USA. PVP2015-45286
24. Shildberg et al., Experimental Determination of the Static Equivalent Pressures of Detonative Explosions of Stoichiometric $CH_4/O_2/N_2$-Mixtures and CH_4/O_2-Mixtures in Long Pipes, Proceedings of ASME 2016, Vancouver, British Columbia, Canada. PVP2016-63223
25. Dorofeev S.B., Hydrogen flames in tubes: critical run-up distances, 2007, ICHS
26. Silvestrini M. et al., Flame acceleration and DDT run-up distances for smooth and obstacle filled tubes. J. Loss Prev. 21, 2008, pp. 555-562
27. Bradley. et al. Flame stretch rate as a determinant of turbulent flame burning velocity, Proceedings of the Royal Society of London, 338, 1992, pp. 359-387
28. Menter F.R., Kuntz M., and Langtry R. (2003). Ten years of industrial experience with the SST turbulence model. Proceedings of the international symposium on turbulence, heat and mass transfer*, 4: 625–632*
29. Gülder O. (1991*)* Turbulent premixed flame propagation models for different combustion regimes. Proc. Combust. Inst. 23, pp. 743-750